Published in final edited form as:
Clin Exp Pharmacol Physiol. 2017 February ; 44(2): 197–206. doi:10.1111/1440-1681.12701.

Connexin32 deficiency is associated with liver injury, inflammation and oxidative stress in experimental non-alcoholic steatohepatitis

Taynã Cristina Tiburcio[#1], **Joost Willebrords**[#2], **Tereza Cristina da Silva**[1], **Isabel Veloso Alves Pereira**[1], **Marina Sayuri Nogueira**[3], **Sara Crespo Yanguas**[2], **Michaël Maes**[2], **Elisangela dos Anjos Silva**[1], **Maria Lucia Zaidan Dagli**[1], **Inar Alves de Castro**[3], **Cláudia Pinto Oliveira**[4], **Mathieu Vinken**[2,*], and **Bruno Cogliati**[1,*]

[1]Department of Pathology, School of Veterinary Medicine and Animal Science, University of São Paulo, Av. Prof. Dr. Orlando Marques de Paiva 87, 05508-270 São Paulo, Brazil

[2]Department of *In Vitro* Toxicology and Dermato-Cosmetology, Faculty of Medicine and Pharmacy, Vrije Universiteit Brussel, Laarbeeklaan 103, 1090 Brussels, Belgium

[3]Department of Food and Experimental Nutrition, Faculty of Pharmaceutical Sciences, University of São Paulo, Av. Prof. Lineu Prestes 580, São Paulo, Brazil

[4]Department of Gastroenterology, Clinical Division, Hepatology Branch, University of São Paulo School of Medicine, Av. Dr. Arnaldo 455, São Paulo, Brazil

[#] These authors contributed equally to this work.

Abstract

Non-alcoholic steatohepatitis is a highly prevalent liver pathology featured by hepatocellular fat deposition and inflammation. Connexin32, which is the major building block of hepatocellular gap junctions, has a protective role in hepatocarcinogenesis and is downregulated in chronic liver diseases. However, the role of connexin32 in non-alcoholic steatohepatitis remains unclear. Connexin32$^{-/-}$ mice and their wild-type littermates were fed a choline-deficient high-fat diet. The manifestation of non-alcoholic steatohepatitis was evaluated based on a battery of clinically relevant read-outs, including histopathological examination, diverse indicators of inflammation and liver damage, in-depth lipid analysis, assessment of oxidative stress, insulin and glucose tolerance, liver regeneration and lipid-related biomarkers. Overall, more pronounced liver damage, inflammation and oxidative stress were observed in connexin32$^{-/-}$ mice compared to wild-type animals. No differences were found in insulin and glucose tolerance measurements and liver regeneration. However, 2 lipid-related genes, srebf1 and fabp3, were upregulated in Cx32$^{-/-}$ mice in comparison with wild-type animals. These findings suggest that connexin32-based signalling is

Contact information: Bruno Cogliati, University of São Paulo, School of Veterinary Medicine and Animal Science, Department of Pathology, Av. Prof. Dr. Orlando Marques de Paiva 87, 05508-270 São Paulo, Brazil. Tel: +551130911200; Fax: +551130917829. bcogliati@usp.br.
[*]These authors share equal seniorship.

Conflict of interest
The authors report no declarations of interest.

Europe PMC Funders Author Manuscripts

not directly involved in steatosis as such, but rather in the *sequela* of this process, which underlie progression of non-alcoholic steatohepatitis.

Keywords

connexin32; inflammation; liver damage; non-alcoholic steatohepatitis; oxidative stress; steatosis

1 Introduction

Non-alcoholic fatty liver disease (NAFLD) covers a spectrum of diseases, ranging from hepatic steatosis to non-alcoholic steatohepatitis (NASH), liver fibrosis, liver cirrhosis and eventually hepatocellular carcinoma. At present, NAFLD is one of the most common chronic liver diseases, with as much as 1 billion patients worldwide (1). Liver steatosis, marked as the first stage of NAFLD, is closely associated with obesity, type 2 diabetes mellitus and insulin resistance (2). While steatosis is considered as a benign and reversible event, NASH has the potential to lead to cirrhosis and hepatocellular carcinoma. Up to 25% of liver steatosis patients progress to NASH and approximately 3% of NASH patients develop liver cancer (3). Thus far, the only curative therapy for chronic liver disease is liver transplantation. Moreover, the economic and social burden of NAFLD/NASH is substantial and health care costs are expected to increase considerably in the upcoming years (4). It is therefore clear that there is an urgent need to find new approaches for the clinical treatment of NAFLD/NASH.

Liver steatosis and NAFLD/NASH are driven by a plethora of intracellular signaling cascades, all which are directed towards the deposition of fat, mainly triglycerides, in hepatocytes and the induction of an inflammatory response (5). Much less is known about the involvement of intercellular communication in this process. Direct intercellular communication is mediated by gap junctions. Gap junctions arise from the interaction of 2 hemichannels of adjacent cells, which in turn consist of 6 connexin (Cx) proteins. Today, 21 different connexins have been identified, all which are expressed in a cell-specific way. In liver, hepatocytes mainly produce Cx32, while the non-parenchymal cell population typically harbours Cx43 (6). However, Cx32 production is strongly downregulated in liver disease, while Cx43 expression is usually increased. Indeed, Cx32 protein amounts and hepatic gap junction activity are drastically reduced in acute drug-induced hepatotoxicity, cholestasis, hepatitis, fibrosis, cirrhosis and hepatocellular carcinoma (7). A similar pattern was seen in a rat model of NASH, where Cx32 expression is decreased in animals fed with a methionine-choline-deficient diet (8). Cx32 dominant negative transgenic rats display reduced liver damage in comparison with wild-type (WT) animals when administered prototypical liver toxicants, such as acetaminophen (9) and carbon tetrachloride (10). Although the exact role of Cx32 remains obscure, these data suggest that Cx32-based signaling could aggravate liver injury. By contrast, liver-specific Cx32 dominant negative transgenic mice and whole-body Cx32 dominant negative rats are known to be much more susceptible to both spontaneously occurring and chemically induced hepatocarcinogenesis (11, 12). This rather points to a cytoprotective function of Cx32-based communication in liver. This was recently shown in a rat model of NASH and NASH-related

Europe PMC Funders Author Manuscripts

hepatocarcinogenesis. Specifically, Cx32 deficiency caused increased inflammation, fibrosis and hepatocarcinogenesis during NASH progression (8).

The present study was set up to gain insight into the involvement of Cx32 in NASH. For this purpose, WT and whole body $Cx32^{-/-}$ mice were fed a choline-deficient high-fat diet. The resulting NASH was evaluated based on several clinically relevant parameters.

2 Results

2.1 Effects of Cx32 deficiency on biometric parameters

Choline plays an important role in hepatic β-oxidation as well as in the production and secretion of very low density lipoproteins. Since choline cannot be *de novo* synthesized, it must be included in the diet. Thus, a diet lacking choline causes hepatic steatosis due to increased uptake of fatty acids and altered secretion of very low density lipoproteins (2). Subsequently, NASH is developed, which is accompanied by oxidative stress (13), production of (adipo)cytokines (14) and liver fibrosis (13). As mice fed only a choline-deficient diet do not develop overweight (15), it is usually combined with a high-fat diet, which facilitates the progression to steatosis and obesity. Therefore, C57BL/6 WT (n=11) and $Cx32^{-/-}$ (n=9) mice were fed a choline-deficient high-fat diet for 8 weeks in the present study. No statistically significant differences were observed in body weight between WT mice and $Cx32^{-/-}$ animals (Fig. 1A.). However absolute ($p<0.01$) as well as relative ($p<0.0001$) liver weight were significantly increased in $Cx32^{-/-}$ mice (Fig. 1A.), a result supported by the macroscopic enlarged liver (Fig. 1B.).

2.2 Effects of Cx32 deficiency on serum transaminases, liver histology and regeneration

Alanine aminotransferase (ALT) and aspartate aminotransferase (AST) are routinely used in clinical settings to diagnose liver damage. In this context, significantly elevated serum levels of both ALT ($p<0.05$) and AST ($p<0.01$) were noticed in $Cx32^{-/-}$ mice (n=9) compared to WT animals (n=11) in experimental NASH (Fig. 1D.). These results could point to an increase in liver damage upon dietary NASH induction in $Cx32^{-/-}$ mice. Evaluation of liver biopsy specimens is still considered as the gold standard for diagnosing NASH. In particular, histopathological NASH assessment is typically based on scoring of steatosis, lobular inflammation and hepatocellular ballooning (16). By doing so, only slightly elevated and non-significant scores of steatosis, ballooning and overall NASH were registered for $Cx32^{-/-}$ mice (n=9) *versus* WT animals (n=11) after experimental NASH induction (Fig. 1C.). This was in line with the observation in frozen liver slices, stained by Oil Red O, where larger fat droplets in the hepatocytes of $Cx32^{-/-}$ mice were seen (Fig. 1B.).

2.3 Effects of Cx32 deficiency on glucose and insulin tolerance

It is well known that NAFLD is closely associated with the metabolic syndrome and insulin resistance. Hyperinsulinemia and hyperglycemia, both caused by increased insulin secretion by pancreatic β cells, together with elevated fatty acids trigger the production of glucose and inhibit β-oxidation. This results in the accumulation of triglycerides in the cytosol of hepatocytes (17). Accordingly, intraperitoneal glucose tolerance test (GTT) and insulin tolerance test (ITT) were performed both in WT and $Cx32^{-/-}$ mice. Only slightly decreased

Europe PMC Funders Author Manuscripts

levels and no statistical difference in glucose levels were found in $Cx32^{-/-}$ mice (n=22) after glucose or insulin injection in comparison with WT animals (n=23) (Fig. 1E.).

2.4 Effects of Cx32 deficiency on serum and liver lipids

NASH is characterized by fat deposition in hepatocytes, which results from drastic changes in lipid homeostasis. In particular, liver steatosis is triggered by enhanced *de novo* synthesis of fatty acids, the molecular constituents of triglycerides, as well as their increased hepatic influx from peripheral tissues (2). Significantly higher ($p<0.05$) levels of triglycerides were measured in liver tissue, but not in serum, of NASH-induced $Cx32^{-/-}$ mice (n=9) in comparison with WT animals (n=11). These genetically modified animals also presented considerably higher ($p<0.01$) circulating cholesterol quantities (Fig. 2A.). Analysis of fatty acids composition in the liver showed no significant differences in total fatty acid content between both groups of mice. However, linoleic acid ($p<0.05$) was significantly less present upon Cx32 deficiency (Fig. 2B.).

2.5 Effects of Cx32 deficiency on serum and liver inflammatory cytokines

NASH is highly associated with inflammation, which is driven by both pro-inflammatory cytokines such as interleukin (IL)-1β, IL-6, interferon (IFN)-γ, tumor necrosis factor (TNF)-α and monocyte chemoattractant protein (MCP)1 and anti-inflammatory cytokines (*e.g.* IL-10) (18). For this reason, a number of cytokines, which are considered of relevance for controlling hepatic injury-associated inflammation, were monitored in this study. Hepatic levels of IL-1β, IL-6, IFN-γ and MCP1 were not changed in $Cx32^{-/-}$ animals (n=9) in comparison with WT cohorts (n=11) after receiving the choline-deficient high-fat diet for 8 weeks (Fig. 3.). However, IL-10 levels were significantly lower ($p<0.05$) in $Cx32^{-/-}$ mice while TNF-α levels were significantly higher ($p<0.05$) (Fig. 3.). Furthermore, significantly increased ($p<0.05$) amounts of IFN-γ were noted in serum (Fig. 3.). All together, these findings suggest that Cx32 deficiency leads to a higher manifestation of inflammation in the liver and serum in experimental NASH.

2.6 Effects of Cx32 deficiency on hepatic oxidative stress

NASH is typically associated with the excessive production of reactive oxygen species, which can degrade polyunsaturated lipids. This lipid peroxidation process yields a number of aldehydes, including malondialdehyde (MDA). MDA is a reactive electrophile species that covalently binds to proteins and thus further exacerbates tissue injury. In addition, superoxide dismutase (SOD), an enzyme responsible for catalyzing superoxide anions, is usually upregulated in the presence of reactive oxygen species (19). Glutathione reductase (GR), glutathione peroxidase (GPx) and catalase are typically downregulated in NASH. Therefore, MDA, SOD, GR, GPx and catalase are frequently used as markers of oxidative stress, *in casu* in the context of NASH (20). Significantly higher ($p<0.05$) liver levels of MDA were detected in $Cx32^{-/-}$ animals (n=9) compared to WT counterparts (n=11) (Fig. 4.). SOD levels were decreased in liver, yet no statistical difference was found between $Cx32^{-/-}$ mice (n=9) and WT cohorts (n=11). Also, no variations were observed among GR, GPx and catalase levels (Fig. 4.). Overall, this indicates a more prominent oxidative stress response to NASH induction in case of lack of Cx32, which as such is in line with the more pronounced liver damage and inflammatory reaction.

2.7 Effects of Cx32 deficiency on serum and fat leptin and adiponectin

Leptin is a key regulator of lipid storage by adjusting the sensation of hunger. Moreover, it has a potential dual action in NAFLD, exerting possible anti-steatotic, but also pro-inflammatory and profibrogenic effects (21). Adiponectin plays an important role in the regulation of lipid homeostasis. Additionally, it enhances glucose utilization and hepatic fatty acid oxidation *via* its receptors, AdipoR1 and AdipoR2. NAFLD patients display low adiponectin levels along with insulin resistance (22). Expression of both proteins is often found to be altered in steatotic mice (2). Levels of leptin and adiponectin were measured in serum from WT (n=11) and $Cx32^{-/-}$ (n=9) animals fed a choline-deficient high-fat diet. No difference was found in serum, but significantly lower levels of leptin ($p<0.01$) and adiponectin ($p<0.05$) were seen in fat tissue (Fig. 4.).

2.8 Effects of Cx32 deficiency on liver regeneration and hepatic key genes involved in NAFLD mechanisms

Dividing cells abundantly produce proliferating cell nuclear antigen (PCNA), a cofactor of DNA polymerase necessary for DNA synthesis and repair (23). Therefore, PCNA expression is commonly used as an indicator of regenerative activity in hepatic tissue following injury. No difference in PCNA levels were found between $Cx32^{-/-}$ (n=9) and WT animals (n=11) (Fig. 5A.). Out of 84 key genes involved in the molecular mechanisms underlying NAFLD, including insulin signaling, adipokine signaling, β-oxidation, cholesterol metabolism, inflammatory response and apoptosis, 4 genes were significantly altered ($p<0.05$) in liver tissue of $Cx32^{-/-}$ mice in comparison with WT animals. These included fatty acid binding protein 3 (encoding for important transporters of long chain fatty acids), sterol regulatory element binding factor 1 (encoding for a transcription factor that controls cholesterol homeostasis by regulating transcription of sterol-regulated genes), insulin-like growth factor binding protein 1 and pyruvate dehydrogenase kinase, isoenzyme 4 (Fig. 5B.).

3 Discussion

Today, NAFLD is the most dominant chronic liver disease in Western countries with a prevalence of 20-30%. Additionally, it is closely associated with insulin resistance, diabetes mellitus type 2 and obesity which makes it a worldwide health problem (1, 2).

The present study demonstrates that mice deficient in Cx32 show intensified features of NASH induced by a choline-deficient high-fat diet compared to WT littermates. Specifically, Cx32-/- animals present higher absolute and relative liver weights. This is associated with increased serum cholesterol levels and hepatic triglyceride amounts independent of changes in total fatty acid content. Linoleic acid, a fatty acid shown to reduce body fat in different animal models and humans (24), is considerably underrepresented in livers of $Cx32^{-/-}$ animals. In this respect, reduced linoleic acid content in a lipidomic analysis of NASH subjects was observed (25). The relevance of these findings, showing enhanced as well as diminished NASH-related lipid production in Cx32 deficiency, is unclear. Furthermore, lack of Cx32 in NASH also results in higher amounts of serum AST, ALT and IFN-γ and liver TNF-α and MDA. In fact, IFN-γ is mainly secreted by circulating T-helper cells (26). The observation that IFN-γ is increased in $Cx32^{-/-}$ animals in comparison with WT cohorts in the

serum, but not in liver, could be due to the fact that inflammation was also caused in other tissues deficient in Cx32. T-cell recruitment and IFN-γ release would therefore be augmented in the blood circulation and hence in serum. Specifically, some immunological alterations involving circulating lymphocytes and neutrophils were found in patients with NASH revealing the presence of a particular profile of peripheral immune cells. Inzaugarat et al. (2011) described an increased frequency of IFN-γ-producing CD4-positive T-cells and also a higher frequency of IFN-γ-producing CD8-positive T-cells in patients with NASH (27). This was paralleled by concomitant lower liver levels of IL-10. Furthermore, levels of lipid-related proteins, such as adiponectin and leptin were not altered in serum but were decreased in fat tissue. Low adiponectin levels are commonly associated with NAFLD and are linked to intrahepatic fat deposition (22). Thus far, Cx32 presence in adipose tissue was not proven. Consequently, the role of Cx32 in fat tissue remains unclear. Additionally, genes such as fatty acid binding protein 3 and sterol regulatory element-binding protein 1 were increased in liver tissue in $Cx32^{-/-}$ mice. Their translated proteins regulate fatty acid synthesis and thus play an important role in the development of NASH (28), which is increased in $Cx32^{-/-}$ mice in this study.

Collectively, these observations point towards more pronounced liver damage, inflammation and oxidative stress upon absence of Cx32. This was also recently shown in Cx32 dominant negative transgenic and WT rats which were given diethylnitrosamine and fed a methionine-choline-deficient diet and developed NASH. Similarly as in this study, Cx32 dominant negative transgenic rats developed more severe liver damage, steatosis, inflammation, fibrosis and oxidative stress. Specifically, hepatic fibrosis was more extensive in Cx32 dominant negative transgenic rats in comparison with WT animals, shown by α-smooth muscle actin staining. Even cirrhosis with bridging fibrosis was found in some Cx32 dominant negative transgenic rats, containing many myofibroblasts within the collagen band in liver (8).

All together, these study results could suggest that Cx32-based signaling is not directly involved in fat deposition and thus steatosis as such, but rather in *sequela* of this process, which underlie NASH progression. Carbenoxolone, an established inhibitor of connexin-based channels and gap junction communication, prevents the development of fatty liver in C57BL/6-Lep *ob/ob* mice by decreasing plasma triglyceride and free fatty acid accumulation, and through downregulation of pro-inflammatory cytokine levels (29). Similarly, carbenoxolone reduces body fat percentage, glycogen content, hypertriglyceridemia, hypercholesterolemia, insulin resistance, adipocyte hypertrophy, adipose tissue inflammation and fibrosis in obese rats (30). These reports indicate that hepatic connexin-mediated communication facilitates liver steatosis and hence NASH, which is in contrast to the findings of the present study. However, these reported results should be considered with caution, as carbenoxolone exerts pleiotropic effects and has several other targets in addition to connexin-based channels (31). On the other hand, genetically modified connexin animals do not allow distinguishing between gap junctions, hemichannels and channel-independent actions of connexins. Regarding this, it has become clear in the past decade that hemichannels are much more than merely acting as structural precursors of gap junctions, as they can also provide a pathway for communication between the cytosol and the extracellular environment. Additionally, connexins can affect

homeostasis independently of their role as building blocks of either gap junctions or hemichannels (32). It remains to be established to what extent each of these connexin communication mechanisms contribute to the outcome of the present study. Anyhow, the results of this study may suggest that boosting of Cx32 expression might be a way to therapeutically reduce the clinical manifestation of NASH.

4 Methods and materials

4.1 Animals and diet treatment

8-week old male C57BL/6 WT and $Cx32^{-/-}$ mice were used in this study, and were housed in the animal facility of the Department of Pathology, School of Veterinary Medicine and Animal Science of the University of São Paulo. $Cx32^{-/-}$ mice were kindly provided by Dr. Klaus Willecke and were backcrossed with WT C57BL/6 mice and genotype was controlled as described previously (33). The animals were kept in a room with ventilation, relative humidity, controlled temperature and light/dark cycle 12:12, and were given water and a choline-deficient high-fat diet (*i.e.* 35% total fat and 54% trans fatty enriched, Rhoster, Brazil) *ad libitum*. Mice were weighed weekly and euthanized after 8 weeks by isoflurane-induced anesthesia and exsanguination during sampling. Blood samples were drawn into heparinized syringes and centrifuged for 10 minutes at 1503*xg*. Serum was stored at -20°C. The liver as well as retroperitoneal and epididymal fat tissue of each animal were weighed and the liver was photographed. Relative liver and fat tissue weights were calculated. Liver fragments were fixed in phosphate-buffered formalin or snap-frozen in liquid nitrogen with storage at -80°C. This study has been approved by the Committee on Bioethics of the School of Veterinary Medicine and Animal Science of the University of São Paulo (Protocol number 9999100314) and all animals received humane care according to the criteria outlined in the “Guide for the Care and Use of Laboratory Animals”.

4.2 Intraperitoneal glucose tolerance and insulin tolerance test

GTT and ITT tests were performed after 8 weeks of choline-deficient high-fat diet to detect disturbances in glucose metabolism. For GTT, mice were fasted for 16 hours, weighed and baseline tail blood glucose measurements were performed. A glucose solution was prepared in sterile phosphate-buffered saline and administered by intraperitoneal injection at 2g/kg body weight. Glucose concentrations were measured in tail blood with an Accu-Chek® Performa glucometer (Roche, Germany) after 0, 30, 60, 90 and 120 minutes. ITT was performed after 48 hours. For this, mice were fasted for 4 hours, weighed and baseline blood glucose measurements were carried out. Human regular insulin (recombinant DNA origin, Humulin R U-100, Brazil) was administered to each mouse *via* intraperitoneal injection at 0.75 units/kg body weight. Blood glucose measurements were performed 0, 30, 60, 90 and 120 minutes after insulin administration.

4.3 Histopathological examination

Liver tissue samples were fixed in 10% formalin for 24 hours and embedded in paraffin wax. The samples were cut into 5 μm sections and stained with hematoxylin and eosin for evaluation of steatosis, hepatocellular ballooning and lobular inflammation as previously described (16). Triglyceride liver accumulation was examined by Oil Red-O staining.

4.4 Analysis of serum aminotransaminases, triglycerides and cholesterol

ALT, AST, triglycerides and cholesterol were measured by a bench-top dry chemistry analyzer (Vet-Test 8008 QBC Analyzer, IDEXX Laboratories Ltd, UK). Results were expressed in IU/L for AST and ALT, and mg/dL for triglycerides and cholesterol serum levels.

4.5 Analysis of hepatic proliferating cell nuclear antigen

Protein expression of PCNA was studied by immunoblotting as described elsewhere (33). Protein concentrations were determined by the Bradford procedure (34) by using a commercial kit (Bio-Rad, USA) with bovine serum albumin as a standard. Proteins were separated on 12% Mini-PROTEAN TGX Precast Protein Gels (Bio-Rad, USA) under reducing conditions and transferred to nitrocellulose membranes with iBlot® Transfer Stacks (Life Technologies, USA). Membranes were incubated with a mouse monoclonal anti-PCNA antibody (Santa Cruz, USA) overnight at 4°C and incubated with a secondary horseradish peroxidase-coupled anti-mouse antibody (Dako, USA) at room temperature for 1 hour. Enhanced chemiluminescence was used to visualize proteins (Amersham Biosciences, USA). Densitometric analysis was performed with a GS170 Calibrated Imaging Densitometer (Bio-Rad, USA). For semi-quantification purposes, PCNA signals were normalized against β-actin signals (Sigma, USA) and expressed as relative alterations compared to WT animals.

4.6 Analysis of inflammatory cytokines, insulin, leptin and adiponectin

Liver and fat fragments were homogenized in lysis buffer with protease inhibitors (Roche, Germany). Homogenates were centrifuged at 14000*xg* for 15 minutes at 4°C and protein concentrations in supernatants were determined by the Bradford procedure (34) using a commercial kit (Bio-Rad, USA) with bovine serum albumin as a standard. Enzyme-linked immunosorbent assay (ELISA) kits were used to measure levels of mouse IL-1β, IL-6, IL-10, IFN-γ, *MCP1*, and TNF-α (BD Biosciences, USA) in liver and serum as previously described (33). Mouse leptin and adiponectin (RD Systems, USA) were measured in serum and fat tissue.

4.7 Analysis of liver triglycerides

Liver lipids were extracted by Folch's method (35). Liver tissue was homogenized in a 2:1 chloroform/methanol solution and shaken at 22°C for 1 hour. The extract was washed with 200 μL deionized water, dried overnight and resuspended in 400 μL butyl alcohol. For quantification of triglycerides, 10 μL of each sample was added to 1 mL Triglyceride Working Reagent (Sigma, USA) in a cuvette. For this purpose, 10 μL water and 10 μL glycerol were used as blank and standard, respectively. All solutions were gently mixed and incubated for 5 minutes at 37°C. Using a Varioskan Flash spectral scanning multimode plate reader, absorbance of each solution was measured at 540 nm (Thermo Fisher Scientific, USA).

4.8 Analysis of liver fatty acids composition

Total lipids were extracted from liver samples and esterified as described by Shirai and group (36). The recovered lipids were reconstituted in 0.5 mL iso-octane. Quantification of fatty acids was performed by gas chromatography (GC) using a G3243A mass spectrometry detector (Agilent 7890 A GC System, Agilent technologies Inc., USA). A fused silica capillary column (J&W DB-23 Agilent 122-236; 60 mm x 250 mm inner diameter) was used for injection of 1 μL of sample. High-purity helium was used as carrier gas at a flow rate of 1.3 mL/minute with a split injection of 50:1. The GC temperature increased gradually from 80°C to 175°C at a rate of 5°C⁄minute, followed by another gradient of 3°C/minute to 230°C for 5 minutes. The temperature of GC inlet and transfer line was 250°C and 280°C, respectively. GC-mass spectrometry was performed using 70 eV electron-ionization in scan acquisition and quantified by total ion current. The fatty acids were identified by the National Institute of Standards and Technology 11 database and their retention times were compared with those of 4 purified standard mixtures of fatty acid methyl esters (Sigma, USA). All mass spectra were acquired over the m/z range of 40-500. Samples were analyzed in triplicate and results were expressed as mg⁄100 mg of hepatic tissue.

4.9 Analysis of liver malondialdehyde

MDA levels in liver protein extracts were measured by reverse phase high-performance liquid chromatography according to the protocol introduced by Hong and co-workers (37). Thiobarbituric acid-MDA conjugate derivative was injected into a Phenomenex reverse-phase C18 analytical column (250 mm x 4.6 mm; 5 mm Phenomenex, USA) with a LC8-D8 pre-column (Phenomenex, USA) and was fluorometrically quantified at an excitation wave length of 515 nm and an emission wave length of 553 nm. The pump delivered the isocratic mobile phase, namely 60% phosphate-buffered saline (10 mmol, pH 7.4) and 40% methanol at a flow rate of 1.0 mL/minute. A standard curve was prepared using 1,1,3,3-tetraetoxipropano. The results were expressed as μmol MDA/mg protein.

4.10 Analysis of liver anti-oxidative enzymes

SOD activity in liver homogenates was determined using a microassay described by Ewing and Janero (38). The SOD scavenging of superoxide anion radical expressed in U/mg protein was calculated by interpolation of the percentage of inhibition of the formazan formation using a linear regression prepared with SOD from bovine erythrocytes (Sigma, USA). Determination of GPx activity was performed using the procedure outlined by Flohé and Günzler (39). Tert-butylhydroperoxide was used as substrate and the formation of oxidized glutathione was monitored spectrophotometrically through nicotinamide adenine dinucleotide phosphate consumption at 340 nm over 4 minutes at 37°C. GPx activity was expressed in U/mg protein and calculated by a linear regression using the percentage of inhibition promoted by glutathione peroxidase (Sigma, USA.). Determination of GR activity was performed as described by Carlberg and Mannervik (40). GR activity expressed U/mg protein was calculated by a linear regression using the percentage of inhibition of nicotinamide adenine dinucleotide phosphate oxidation promoted by GR (Sigma, USA). Catalase activity was determined according to Bonaventura and co-workers (41). Liver homogenate containing 0.05 μg/μL of protein (*i.e.* 20 μL) was added to a microplate with

140 μL phosphate-buffered saline (*i.e.* 50 mM with 0.1 mM ethylenediamine tetra-acetic acid, pH 7.4) and 40 μL 30 mM freshly prepared hydrogen peroxide. The absorbance was continuously monitored over 8 minutes at 30°C at 240 nm. A standard curve was prepared using catalase enzyme (Sigma USA).

4.11 cDNA expression array

Quantitative real-time polymerase chain reaction (qRT-PCR) analysis was performed following the MIQE guidelines (42). Total RNA was extracted from liver tissue using an RNAspin Mini RNA Isolation Kit (GE HealthCare, USA) according to the manufacturer's guidelines. Purity and quantification of isolated RNA were measured spectrophotometrically using a Nanodrop spectrophotometer (Thermo Scientific, USA). A cut-off ratio between 1.5 and 2.0 for the absorption at 260/280 nm was used for assessing purity. Then, 3 μg total RNA was reverse-transcribed using Taqman Reverse Transcription Reagents (Applied Biosystems, USA) to yield cDNA. Gene expression array analysis of liver tissue from WT or $Cx32^{-/-}$ mice fed a choline deficient high-fat diet was performed by Mouse Fatty Liver PCR Array (SABiosciences, USA). Analyses were carried out using a LightCycler 96 Real-Time PCR system (Roche Diagnostic, Germany). Analysis of relative gene expression data was performed according to the $2^{-\Delta\Delta Ct}$ method by Livak and Schmittgen (43). Results were expressed as fold change of ΔΔCt values obtained from WT mice at the respective day of measurement. Modifications in gene expression with fold changes ≥2.0 or ≤-2.0 compared to the reference genes (β2 microglobulin, glucuronidase β and heat shock protein 90 α class B member 1) were considered biologically significant.

4.12 Statistical analysis

The number of repeats (n) for each analysis varied and is specified in the discussion of the results. All data were expressed as mean ± standard error of the mean (SEM). Results were statistically processed by a 2-tailed unpaired student *t*-test and Welch's correction using GraphPad Prism6 software, with probability (p) values of less than or equal to 0.05 considered as significant.

Acknowledgments

This work was financially supported by the grants of the University of São Paulo-Brazil, Coordenação de Aperfeiçoamento de Pessoal de Nível Superior (CAPES), the Fundação de Amparo à Pesquisa do Estado de São Paulo (FAPESP SPEC grant 2013/50420-6), European Research Council (ERC Starting Grant 335476), the Fund for Scientific Research-Flanders (FWO grants G009514N and G010214N) and the University Hospital of the Vrije Universiteit Brussel-Belgium ("Willy Gepts Fonds" UZ-VUB).

List of abbreviations

ALT	alanine aminotransferase
AST	aspartate aminotransferase
Cx	connexin
ELISA	enzyme-linked immunosorbent assay
GC	gas chromatography

Europe PMC Funders Author Manuscripts

GPx	glutathione peroxidase
GR	glutathione reductase
GTT	glucose tolerance test
IFN-γ	interferon-γ
IL-1β/6/10/18	interleukin 1β/6/10/18
ITT	insulin tolerance test
MCP1	monocyte chemoattractant protein 1
MDA	malondialdehyde
n	number of repeats
NAFLD	non-alcoholic fatty liver disease
NASH	non-alcoholic steatohepatitis
p	probability
PCNA	proliferating cell nuclear antigen
SEM	standard error of the mean
SOD	superoxide dismutase
TNF-α	tumor necrosis factor α
WT	wild-type

References

1. Loomba R, Sanyal AJ. The global NAFLD epidemic. Nat Rev Gastroenterol Hepatol. 2013; 10:686–90. [PubMed: 24042449]
2. Willebrords J, Pereira IV, Maes M, et al. Strategies, models and biomarkers in experimental non-alcoholic fatty liver disease research. Prog Lipid Res. 2015; 59:106–25. [PubMed: 26073454]
3. Schuppan D, Schattenberg JM. Non-alcoholic steatohepatitis: pathogenesis and novel therapeutic approaches. J Gastroenterol Hepatol. 2013; 28(Suppl 1):68–76.
4. Corey KE, Kaplan LM. Obesity and liver disease: the epidemic of the twenty-first century. Clin Liver Dis. 2014; 18:1–18. [PubMed: 24274861]
5. Peverill W, Powell LW, Skoien R. Evolving concepts in the pathogenesis of NASH: beyond steatosis and inflammation. Int J Mol Sci. 2014; 15:8591–638. [PubMed: 24830559]
6. Maes M, Decrock E, Cogliati B, et al. Connexin and pannexin (hemi)channels in the liver. Front Physiol. 2014; 4:405. [PubMed: 24454290]
7. Vinken M. Gap junctions and non-neoplastic liver disease. J Hepatol. 2012; 57:655–62. [PubMed: 22609308]
8. Sagawa H, Naiki-Ito A, Kato H, et al. Connexin 32 and luteolin play protective roles in non-alcoholic steatohepatitis development and its related hepatocarcinogenesis in rats. Carcinogenesis. 2015

9. Naiki-Ito A, Asamoto M, Naiki T, et al. Gap junction dysfunction reduces acetaminophen hepatotoxicity with impact on apoptotic signaling and connexin 43 protein induction in rat. Toxicol Pathol. 2010; 38:280–6. [PubMed: 20097795]
10. Asamoto M, Hokaiwado N, Murasaki T, Shirai T. Connexin 32 dominant-negative mutant transgenic rats are resistant to hepatic damage by chemicals. Hepatology. 2004; 40:205–10. [PubMed: 15239104]
11. Dagli ML, Yamasaki H, Krutovskikh V, Omori Y. Delayed liver regeneration and increased susceptibility to chemical hepatocarcinogenesis in transgenic mice expressing a dominant-negative mutant of connexin32 only in the liver. Carcinogenesis. 2004; 25:483–92. [PubMed: 14688024]
12. Kato H, Naiki-Ito A, Naiki T, et al. Connexin 32 dysfunction promotes ethanol-related hepatocarcinogenesis via activation of Dusp1-Erk axis. Oncotarget. 2015
13. Leclercq IA, Farrell GC, Field J, Bell DR, Gonzalez FJ, Robertson GR. CYP2E1 and CYP4A as microsomal catalysts of lipid peroxides in murine nonalcoholic steatohepatitis. J Clin Invest. 2000; 105:1067–75. [PubMed: 10772651]
14. Larter CZ, Yeh MM, Williams J, Bell-Anderson KS, Farrell GC. MCD-induced steatohepatitis is associated with hepatic adiponectin resistance and adipogenic transformation of hepatocytes. J Hepatol. 2008; 49:407–16. [PubMed: 18534710]
15. Rinella ME, Elias MS, Smolak RR, Fu T, Borensztajn J, Green RM. Mechanisms of hepatic steatosis in mice fed a lipogenic methionine choline-deficient diet. J Lipid Res. 2008; 49:1068–76. [PubMed: 18227531]
16. Kleiner DE, Brunt EM, Van Natta M, et al. Design and validation of a histological scoring system for nonalcoholic fatty liver disease. Hepatology. 2005; 41:1313–21. [PubMed: 15915461]
17. Pettinelli P, Obregón AM, Videla LA. Molecular mechanisms of steatosis in nonalcoholic fatty liver disease. Nutr Hosp. 2011; 26:441–50. [PubMed: 21892559]
18. Duwaerts CC, Maher JJ. Mechanisms of Liver Injury in Non-Alcoholic Steatohepatitis. Curr Hepatol Rep. 2014; 13:119–29. [PubMed: 25045618]
19. Laurent A, Nicco C, Tran Van Nhieu J, et al. Pivotal role of superoxide anion and beneficial effect of antioxidant molecules in murine steatohepatitis. Hepatology. 2004; 39:1277–85. [PubMed: 15122756]
20. Basaranoglu M, Basaranoglu G, Sentürk H. From fatty liver to fibrosis: a tale of “second hit”. World J Gastroenterol. 2013; 19:1158–65. [PubMed: 23483818]
21. Polyzos SA, Kountouras J, Mantzoros CS. Leptin in nonalcoholic fatty liver disease: a narrative review. Metabolism. 2015; 64:60–78. [PubMed: 25456097]
22. Giby VG, Ajith TA. Role of adipokines and peroxisome proliferator-activated receptors in nonalcoholic fatty liver disease. World J Hepatol. 2014; 6:570–9. [PubMed: 25232450]
23. Theocharis SE, Skopelitou AS, Margeli AP, Pavlaki KJ, Kittas C. Proliferating cell nuclear antigen (PCNA) expression in regenerating rat liver after partial hepatectomy. Dig Dis Sci. 1994; 39:245–52. [PubMed: 7906221]
24. Park Y, Albright KJ, Liu W, Storkson JM, Cook ME, Pariza MW. Effect of conjugated linoleic acid on body composition in mice. Lipids. 1997; 32:853–8. [PubMed: 9270977]
25. Puri P, Wiest MM, Cheung O, et al. The plasma lipidomic signature of nonalcoholic steatohepatitis. Hepatology. 2009; 50:1827–38. [PubMed: 19937697]
26. Narayanan S, Surette FA, Hahn YS. The Immune Landscape in Nonalcoholic Steatohepatitis. Immune Netw. 2016; 16:147–58. [PubMed: 27340383]
27. Inzaugarat ME, Ferreyra Solari NE, Billordo LA, Abecasis R, Gadano AC, Cherñavsky AC. Altered phenotype and functionality of circulating immune cells characterize adult patients with nonalcoholic steatohepatitis. J Clin Immunol. 2011; 31:1120–30. [PubMed: 21845516]
28. Sharma M, Mitnala S, Vishnubhotla RK, Mukherjee R, Reddy DN, Rao PN. The Riddle of Nonalcoholic Fatty Liver Disease: Progression From Nonalcoholic Fatty Liver to Nonalcoholic Steatohepatitis. J Clin Exp Hepatol. 2015; 5:147–58. [PubMed: 26155043]
29. Rhee SD, Kim CH, Park JS, et al. Carbenoxolone prevents the development of fatty liver in C57BL/6-Lep ob/ob mice via the inhibition of sterol regulatory element binding protein-1c activity and apoptosis. Eur J Pharmacol. 2012; 691:9–18. [PubMed: 22742899]

30. Prasad Sakamuri SS, Sukapaka M, Prathipati VK, et al. Carbenoxolone treatment ameliorated metabolic syndrome in WNIN/Ob obese rats, but induced severe fat loss and glucose intolerance in lean rats. PLoS One. 2012; 7:e50216. [PubMed: 23284633]
31. Bodendiek SB, Raman G. Connexin modulators and their potential targets under the magnifying glass. Curr Med Chem. 2010; 17:4191–230. [PubMed: 20939816]
32. Vinken M, Decrock E, Leybaert L, et al. Non-channel functions of connexins in cell growth and cell death. Biochim Biophys Acta. 2012; 1818:2002–8. [PubMed: 21718687]
33. Maes M, McGill MR, da Silva TC, et al. Connexin32: a mediator of acetaminophen-induced liver injury? Toxicol Mech Methods. 2016:1–9. [PubMed: 26275125]
34. Bradford MM. A rapid and sensitive method for the quantitation of microgram quantities of protein utilizing the principle of protein-dye binding. Anal Biochem. 1976; 72:248–54. [PubMed: 942051]
35. Folch J, Lees M, Sloane Stanley GH. A simple method for the isolation and purification of total lipides from animal tissues. J Biol Chem. 1957; 226:497–509. [PubMed: 13428781]
36. Shirai N, Suzuki H, Wada S. Direct methylation from mouse plasma and from liver and brain homogenates. Anal Biochem. 2005; 343:48–53. [PubMed: 15964541]
37. Hong YL, Yeh SL, Chang CY, Hu ML. Total plasma malondialdehyde levels in 16 Taiwanese college students determined by various thiobarbituric acid tests and an improved high-performance liquid chromatography-based method. Clin Biochem. 2000; 33:619–25. [PubMed: 11166008]
38. Ewing JF, Janero DR. Microplate superoxide dismutase assay employing a nonenzymatic superoxide generator. Anal Biochem. 1995; 232:243–8. [PubMed: 8747482]
39. Flohé L, Günzler WA. Assays of glutathione peroxidase. Methods Enzymol. 1984; 105:114–21. [PubMed: 6727659]
40. Carlberg I, Mannervik B. Purification and characterization of the flavoenzyme glutathione reductase from rat liver. J Biol Chem. 1975; 250:5475–80. [PubMed: 237922]
41. Bonaventura J, Schroeder WA, Fang S. Human erythrocyte catalase: an improved method of isolation and a reevaluation of reported properties. Arch Biochem Biophys. 1972; 150:606–17. [PubMed: 5044042]
42. Bustin SA, Benes V, Garson JA, et al. The MIQE guidelines: minimum information for publication of quantitative real-time PCR experiments. Clin Chem. 2009; 55:611–22. [PubMed: 19246619]
43. Livak KJ, Schmittgen TD. Analysis of relative gene expression data using real-time quantitative PCR and the 2(-Delta Delta C(T)) Method. Methods. 2001; 25:402–8. [PubMed: 11846609]

Europe PMC Funders Author Manuscripts

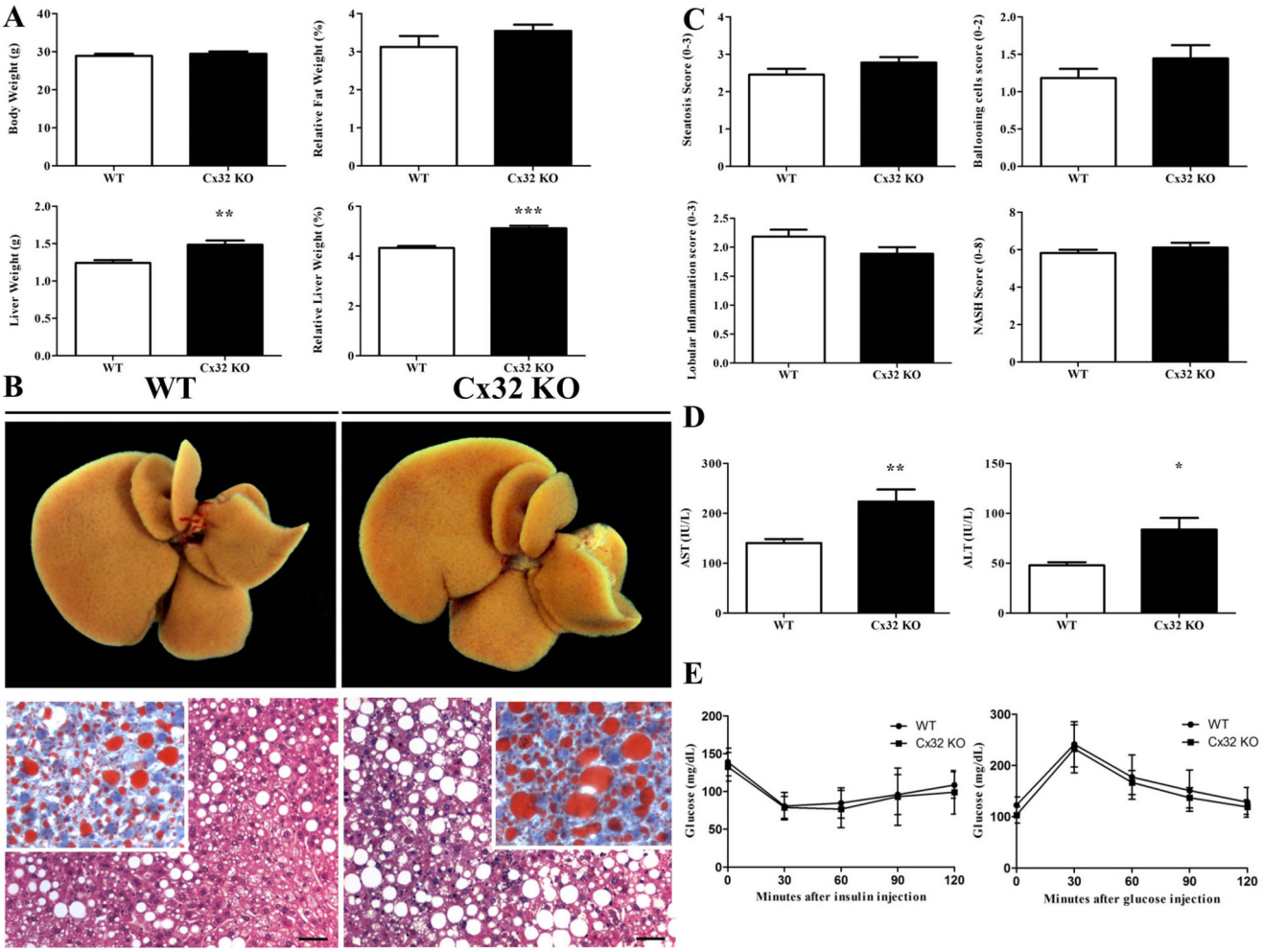

Figure 1. Effects of Cx32 deficiency on biometric parameters, macroscopic and microscopic liver appearance, and glucose and insulin tolerance.

WT (n=11) and Cx32$^{-/-}$ (n=9) mice were fed a high-fat choline-deficient diet for 8 weeks before sampling. **(A)** Body, fat and liver of WT and Cx32$^{-/-}$ mice were weighed. **(B)** Macroscopic pictures (upper panels) of liver and microscopic pictures (lower panels) of HE and Oil red staining were taken. **(C)** Steatosis, lobular inflammation and ballooning was graded and NASH score was determined. **(D)** ALT and AST were measured in the serum of Cx32$^{-/-}$ and WT animals. **(E)** GTT and ITT were performed by injecting glucose and insulin respectively, both in Cx32$^{-/-}$ (n=22) and WT (n=23) mice. Glucose levels were measured every 30 minutes for 120 minutes. Data are expressed as means ± SEM with **p<0.01 and ***p<0.0001.

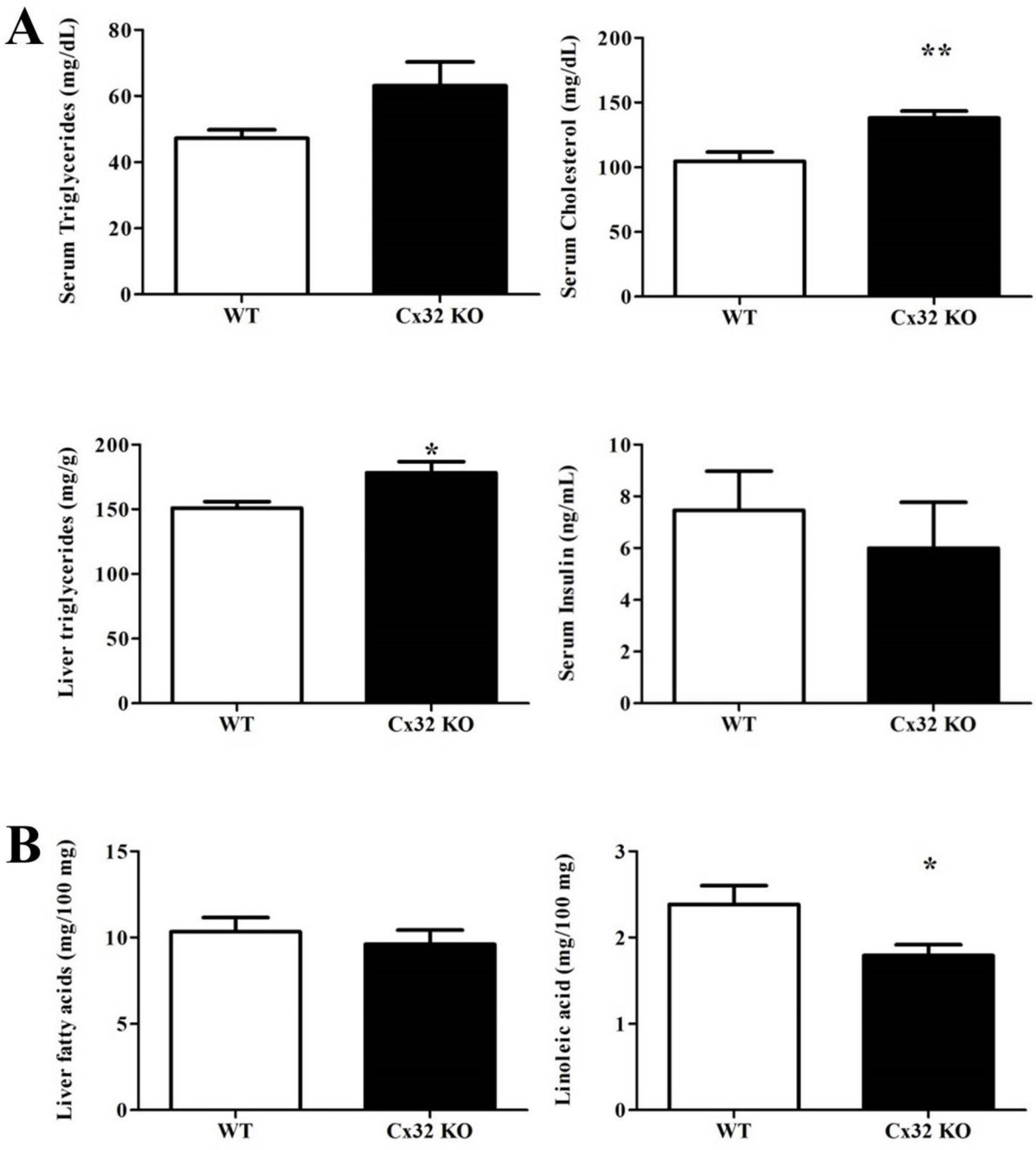

Figure 2. Effects of Cx32 deficiency on lipid content.

WT (n=11) and Cx32$^{-/-}$ (n=9) mice were fed a high-fat choline-deficient diet for 8 weeks before sampling. **(A)** Liver triglycerides were spectrophotometrically quantified after extraction. Serum triglycerides, cholesterol and insulin were measured. **(B)** Liver fatty acid content and linoleic acid levels were determined by mass spectrometry-GC. Data are expressed as means ± SEM with *p<0.05 and **p<0.01.

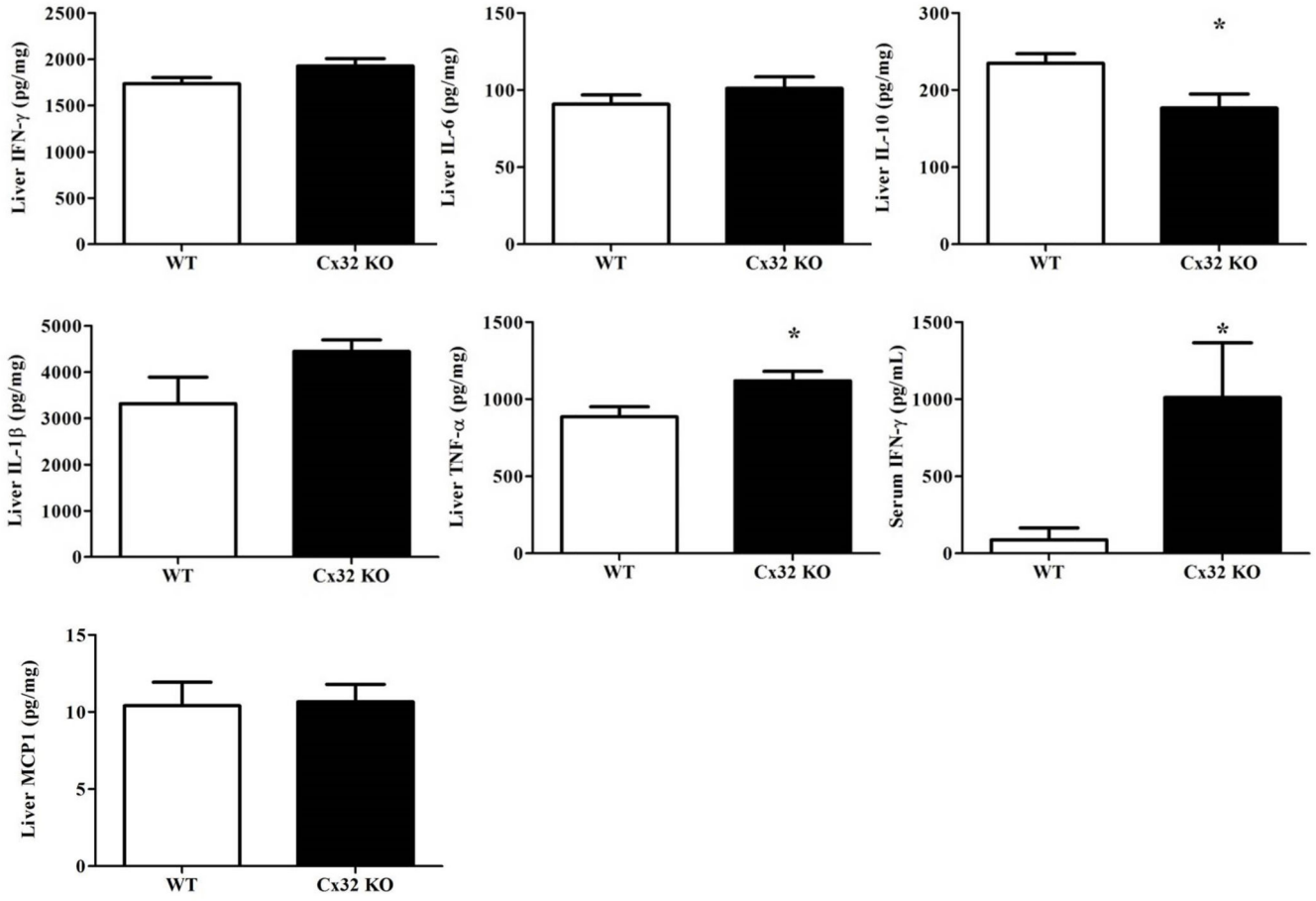

Figure 3. Effects of Cx32 deficiency on inflammatory cytokines.

WT (n=11) and $Cx32^{-/-}$ (n=9) mice were fed a high-fat choline-deficient diet for 8 weeks before sampling. ELISA analysis of IFN-γ, IL-6, IL-1β, TNF-α and IL-10 in liver tissue and serum was performed. Data are expressed as means ± SEM with *p<0.05, **p<0.01 and ***p<0.0001.

Europe PMC Funders Author Manuscripts

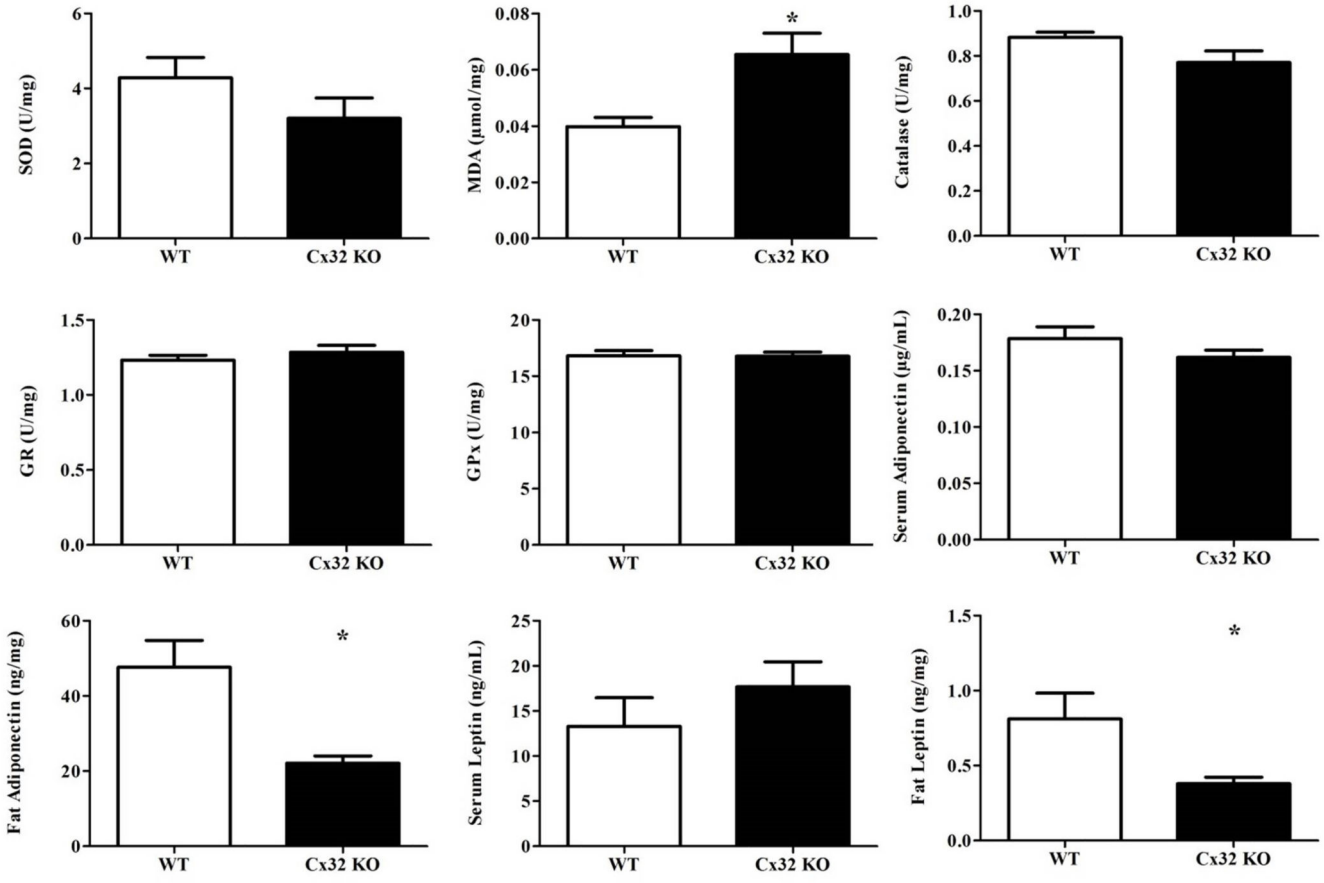

Figure 4. Effects of Cx32 deficiency on oxidative stress, leptin and adiponectin.

WT (n=11) and $Cx32^{-/-}$ (n=9) mice were fed a high-fat choline-deficient diet for 8 weeks before sampling. MDA in liver tissue was measured by high-performance liquid chromatography. Liver superoxide dismutase, glutathione reductase, glutathione peroxidase and catalase levels were determined by their activity by microassay. Adiponectin and leptin in fat and serum were measured by ELISA. Data are expressed as means ± SEM with *$p<0.05$.

Europe PMC Funders Author Manuscripts

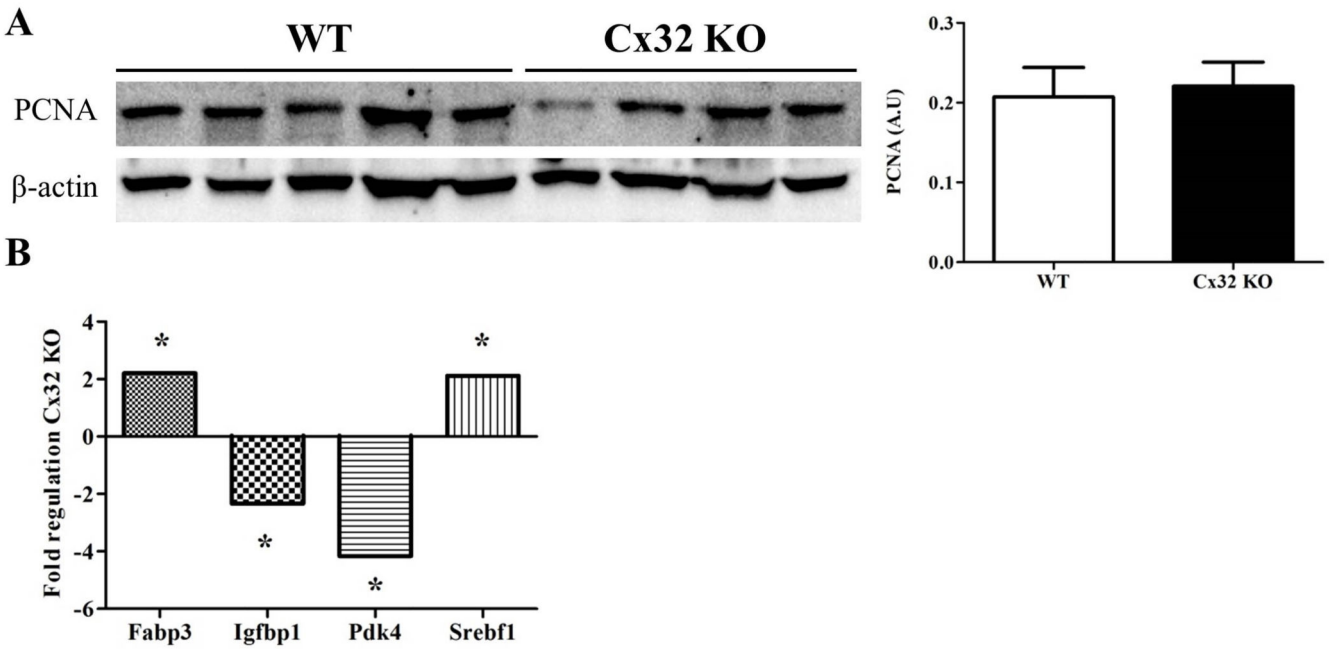

Figure 5. Effects of Cx32 deficiency on PCNA levels and NAFLD-related genes.

(A) PCNA proteins were detected by immunoblotting technique and enhanced chemiluminescence and quantified by densitometric analysis. **(B)** qRT-PCR was performed on 84 key genes related to NAFLD mechanisms. Data are expressed as means ± SEM with *p<0.05.

Europe PMC Funders Author Manuscripts